Reconfiguration of a Nadir-Pointing 2-Craft Coulomb Tether

Arun Natarajan, Hanspeter Schaub and Gordon G. Parker

Reconfiguration of a Nadir-Pointing 2-Craft Coulomb Tether

Arun Natarajan,[*] Hanspeter Schaub[†] and Gordon G. Parker[‡]

Abstract

The linear dynamics and stability analysis of reconfiguring a 2-spacecraft Coulomb tether formation is investigated. In this concept the tether between two craft is replaced with electrostatic force fields. Here the relative distance between the two satellites is increased or decreased using electrostatic Coulomb forces. The two craft are connected by an electrostatic tether which is capable of both tensile and compressive forces. The resulting virtual structure can change its shape by modifying the desired reference length. As a result, the two-craft formation will essentially act as a long, slender, nearly-rigid body of variable length. Inter-spacecraft Coulomb forces cannot influence the inertial angular momentum of this formation. However, the gravity gradient effect can be exploited to stabilize the attitude of this Coulomb tether formation about an orbit radial direction. Limits of the Coulomb tether expansion and contraction rates are discussed using linearized time-varying dynamical models. These allow the reference length time histories to be designed while ensuring linear stability of the virtual structure.

Keywords – Coulomb Tether, Formation Flying

1 Introduction

A new formation flying concept using electrostatic propulsion was introduced in References [1],[2],[3]. The charge of a spacecraft is controlled by active emission of charged particles and this charge transfer is used to generate inter-spacecraft Coulomb forces. These Coulomb forces can be used to control the relative motion of the spacecraft or hold them in rigid formations over short distances ranging 10-100 meters. This novel propellantless relative navigation control concept has many potential advantages over conventional thrusters like ion engines. Coulomb propulsion effectively uses no consumables and enables high precision, close-proxmity formation flying applications. It is also a very clean method of propulsion compared to ion engines, thereby avoiding the thruster plume contamination issue with neighboring crafts. Further, the study of electrostatic charging data of the SCATHA spacecraft[4] verified that spacecraft can charge to very high voltages in low plasma environments such as GEO and the electric power requirement will be typically less than 1 Watt. However, this Coulomb propulsion also has its own set of limitations. The Coulomb electrostatic force magnitude is inversely proportional to the square of the separation distance. Hence, this method is effective only for close formations of the order of 10-100m. Additionally, Coulomb force effectiveness is diminished in a space plasma environment due to the presence of charged plasma particles. The electric field strength drops off exponentially with

---

[*]Graduate Student, Aerospace and Ocean Eng. Dep., Virginia Tech, Blacksburg, VA 24061.

[†]Assistant Professor, Aerospace and Ocean Eng. Dep., Virginia Tech, Blacksburg, VA 24061.

[‡]Associate Professor, Dep. of Mechanical Eng., Michigan Tech, Houghton, MI 49931.

increasing separation distance. The severity of this drop is characterized using the Debye length.[5,6] For low earth orbits (LEO), the Debye length is of the order of millimeters to centimeters, making the Coulomb formation flying concept impractical at these low orbit altitudes. At geostationary orbit (GEO) altitudes or higher, which has a hotter and less dense plasma environment, the Debye length can vary between 100-1000 meters depending on the solar activity cycles. The Coulomb formation flying concept appears to be feasible at this altitude.

King et al. found analytical solutions for Hill-frame invariant Coulomb formations.[2] Here spacecraft are placed at specific locations in the rotating Hill frame with specific electrostatic charges. As a result the Coulomb forces perfectly cancel all Keplerian relative orbit accelerations, causing the satellites to remain fixed or static as seen by the constantly rotating Hill frame. However, the charge is held constant in this early analysis. The discovered open-loop static Coulomb formations were all found to be unstable. Reference 3 discusses these static Coulomb satellite formations and a nonlinear control which is capable of bounding the relative motion between two close craft. This charge feedback control can also be used to control general orbit element differences with guaranteed stability, but not necessarily asymptotic convergence. In References 7, a genetic algorithm for numerically finding the static charges to maintain a multi-craft Coulomb formation is given. The analytical solution for the static charge and their feasibility for different shapes in two and three craft formations are discussed in detail in Reference 8. In Reference 9, a hybrid propulsion system using ion thrusting and Coulomb forces is developed for maintaining a swarm of satellites in formation. Izzo and Pettazzi[10] propose using Coulomb forces for aiding the self assembling of large structures in space. Here, the use of Coulomb forces reduce the propellent consumption significantly. Reference 11 studies the stabilization of a simple static 2-craft Coulomb tether structure aligned along the orbit radial direction. Compared to the previous works on static Coulomb structures, Reference 11 is the first study to introduce a charge feedback law to stabilize a simple Coulomb structure to a specific shape and orientation. Coulomb forces are inter-spacecraft forces and can not control the inertial angular momentum of the formation. Hence, stability characteristics of orbital rigid body motion under a gravity gradient field was applied to a Coulomb tethered two-spacecraft system to develop an active charge feedback control. With this control the spacecraft separation distance can be maintained at a fixed value, while the coupled gravity gradient torque is exploited to stabilize the formation attitude about the orbit nadir vector. Further, as the separation distance converged to the desired value, the in-plane rotation angle is shown to converge to zero as well. The out-of-plane angle is shown to be decoupled from the other modes and not influenced (to first order) by the spacecraft charges.

This paper extends this earlier work by investigating how to reconfigure the 2-craft Coulomb tether formation by forcing the craft to move apart or come closer using the Coulomb force and again using the gravity gradient to stabilize the formation. An active charge feedback law is introduced and the linear stability of the coupled separation distance and attitude is evaluated for this time-variant system. Based on this analysis, stability regions for expanding and contracting the two-craft formation are established. A comprehensive study of the dynamics of physically connected tether systems are presented in Reference 12. Note that contrary to these physically connected tethers, the Coulomb tether is capable of receiving both tensile and compressive forces, resulting in a flexible virtual tether. With Coulomb tether, the problems associated with complex cable dynamics are

avoided thereby making the force to lie along a straight line joining the craft. Further, the stiffness or flexibility of the satellite connection can be controlled through feedback control laws. This will allow for the Coulomb tether stiffness to be varied with changing mission requirements. In References 13 and 14, the dynamics of a physically connected two-craft tether is studied where they develop length rate laws that guarantee stability. The attitude stability that is achieved is only a bounded stability. In the current work, with an electrostatic virtual tether replacing the actual tether, the feedback law attempts to asymptotically stabilize the separation distance and the in-plane oscillations. The asymptotic stability is achievable due to the virtual tether which allows both compression and tension and a flexible tether length. The formation is studied in GEO and the Debye lengths are assumed to be sufficiently large so that the effects of Debye shielding can be neglected. Finally, numerical simulations illustrate the analytical stability predictions.

2   Satellite Reconfiguration Dynamics

A 2-satellite formation is considered as shown in the Figure 1. The center of mass is assumed to maintain a circular Keplerian orbit and the two satellites are nominally aligned along the orbit radial direction. In essence, these two charged spacecraft will behave like a conventional 2-craft tether system, with the exception that this electrostatic tether is capable both of attractive and repulsive forces. Reference 11 shows that the relative distance between the two satellites can be controlled using electrostatic Coulomb forces. A charge feedback law is used to maintain the relative distance at a constant value. As a result, the two satellites behave like a long slender nearly rigid body and the differential gravitational attraction is used to stabilize the attitude of this formation about the orbit radial direction. From this point onwards, this will be referred to as the Coulomb tether regulation problem. These concepts are extended for the time varying Coulomb tether length tracking problem. The main aim in the tracking (reconfiguration) problem is to increase or decrease the relative distance between the satellites by forcing them to move relative to each other along a prescribed path. This static Coulomb structure reconfiguration is to be accomplished without loosing altitude stability.

The Clohessy-Wiltshire-Hill's equations[15, 16, 17] for one of the spacecraft in the 2-craft Coulomb tether formation as shown in Figure 2, is given by

$$\ddot{x}_1 - 2\Omega\dot{y}_1 - 3\Omega^2 x_1 = \frac{k_c}{m_1}\frac{(x_1 - x_2)}{L^3}q_1 q_2 \tag{1a}$$

$$\ddot{y}_1 + 2\Omega\dot{x}_1 = \frac{k_c}{m_1}\frac{(y_1 - y_2)}{L^3}q_1 q_2 \tag{1b}$$

$$\ddot{z}_1 + \Omega^2 z_1 = \frac{k_c}{m_1}\frac{(z_1 - z_2)}{L^3}q_1 q_2 \tag{1c}$$

where $(x_i, y_i, z_i)^T$ is the position vector of the ith satellite in Hill frame components, m_1 and q_1 are the mass and charge of satellite 1, and L is the distance between the satellites 1 and 2. The constant chief orbital rate is given by $\Omega = \sqrt{\mu/r_c^3}$, where μ is the gravitational coefficient and $\boldsymbol{r}_c$ is center of mass position vector. The parameter $k_c = 8.99 \cdot 10^9 \ \text{Nm}^2/\text{C}^2$ is the Coulomb constant. As the Hill frame origin is set to be identical to the formation center of mass, the motion of the 2nd craft can be found by noting that the center of mass
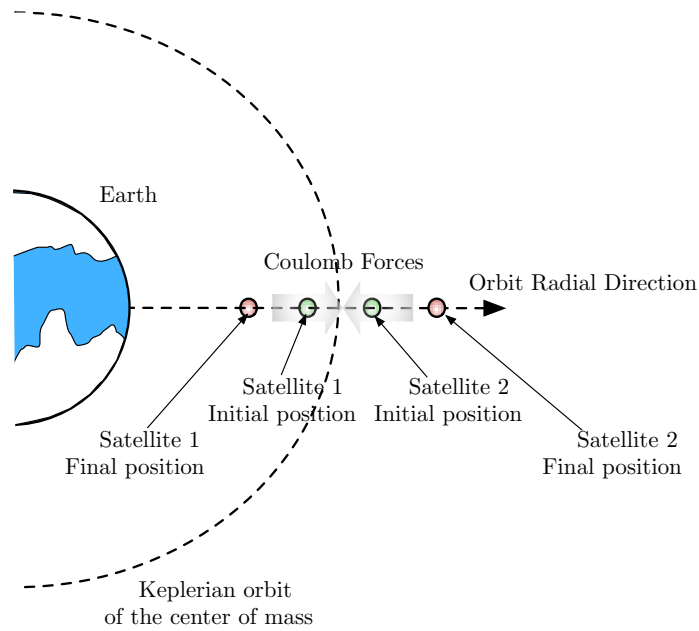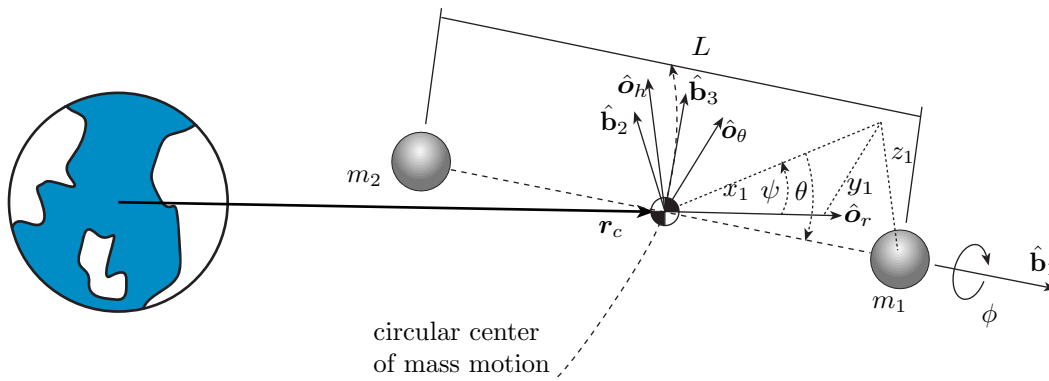
Figure 1: A simple Coulomb tracking illustration.

Figure 2: Coulomb Tethered Two Satellite Formation with the Satellites Aligned Along the Orbit Nadir Direction

vector is constant due to conservation of linear momentum. This yields[18,19]

$$m_1\boldsymbol{\rho}_1 + m_2\boldsymbol{\rho}_2 = 0 \tag{2}$$

The differential equation of the separation distance L, between the two satellites is given by[11]

$$\ddot{L} = (2\Omega\dot{\psi} + 3\Omega^2)L + \frac{k_c}{m_1}Q\frac{1}{L^2}\frac{m_1 + m_2}{m_2} \tag{3}$$

where $\dot{\psi}$ is the angular in-plane perturbation rate and Q is the product of spacecraft charges q_1 and q_2. For the Coulomb tether regulation problem, L is the sum of a constant reference length L_{ref} and a small varying length δL. Similarly, let Q be the sum of Q_{ref}, which is the ideal constant charge product needed to maintain the satellites in a rigid formation of length L_{ref}, and a small charge product variation δQ.

$$L(t) = L_{\mathrm{ref}} + \delta L(t) \tag{4a}$$
$$Q(t) = Q_{\mathrm{ref}} + \delta Q(t) \tag{4b}$$

The reference charge product Q_{ref} is a function of L_{ref} and is computed analytically from the linearized Hill frame equations. The analytical expression for Q_{ref} is written as[11,8]

$$Q_{\mathrm{ref}} = -3\Omega^2\frac{L_{\mathrm{ref}}^3}{k_c}\frac{m_1 m_2}{m_1 + m_2} \tag{5}$$

It should be noted that in the Coulomb tether regulation problem L_{ref} is constant and the differential equation given in Eq. (3) is linearized by assuming a small δL separation distance error. This can be slightly modified to accommodate the Coulomb tracking problem. The reference Coulomb structure length $L_{\mathrm{ref}}(t)$ is made time varying, but the separation distance errors $\delta L(t)$ are still assumed to be small.

$$L(t) = L_{\mathrm{ref}}(t) + \delta L(t) \tag{6a}$$
$$Q(t) = Q_{\mathrm{ref}}(t) + \delta Q(t) \tag{6b}$$

Here $L_{\mathrm{ref}}(t)$ is the time varying reference separation distance and $Q_{\mathrm{ref}}(t)$ is the corresponding reference charge product which can be calculated using Eq. (5). Substituting the assumptions in Eq. (6) into Eq. (3) and linearizing assuming small δL yields

$$\delta\ddot{L} = -\ddot{L}_{\mathrm{ref}} + 2\Omega L_{\mathrm{ref}}\dot{\psi} + 9\Omega^2\delta L + \frac{k_c}{m_1}\delta Q\frac{1}{L_{\mathrm{ref}}^2}\frac{m_1 + m_2}{m_2} \tag{7}$$

This equation establishes the relation between the additional charge product δQ required and the change in relative separation of the satellites. Note that this relation is coupled to the angular in-plane perturbation rate $\dot{\psi}$. In order to obtain an expression for this perturbation, a stability analysis using the gravity gradient is employed. The derivation of the expression for angular perturbation closely follows the derivation given in Reference 11 for the Coulomb regulation problem. The linearized attitude dynamics of the Coulomb

tether body frame are written along with the separation distance equation as:

$$\ddot{\theta} + \frac{2\dot{L}_{\text{ref}}}{L_{\text{ref}}}\dot{\theta} + 4\Omega^2\theta = 0 \tag{8a}$$

$$\ddot{\psi} + \frac{2\dot{L}_{\text{ref}}}{L_{\text{ref}}}\dot{\psi} + \frac{2\Omega}{L_{\text{ref}}}\delta\dot{L} - \frac{2\dot{L}_{\text{ref}}}{L_{\text{ref}}^2}\Omega\delta L + \frac{2\dot{L}_{\text{ref}}}{L_{\text{ref}}}\Omega + 3\Omega^2\psi = 0 \tag{8b}$$

$$\delta\ddot{L} + \ddot{L}_{\text{ref}} - 2\Omega L_{\text{ref}}\dot{\psi} - 9\Omega^2\delta L - \frac{k_c}{m_1}\delta Q\frac{1}{L_{\text{ref}}^2}\frac{m_1 + m_2}{m_2} = 0 \tag{8c}$$

Thus, Eq. (8a) – (8c) are the linearized equations of motion of the Coulomb tracking about the static nadir reference configuration. These equations of motion are similar to the ones developed for the physically connected tether systems in Reference 12, with tension in the cable replaced by Coulomb force. One key difference between the equations of motion for the physically connected tether system and Coulomb tracking is in the linearization of separation distance. Due to the inherent flexibility present in the virtual Coulomb tether, the separation distance can be modeled as a sum of required separation distance (L_{ref}) and a small separation distance error (δL), and the equations of motion are linearized for small δL. Such linearization technique is not commonly encountered in physically connected tether systems. In Eq. (8a) – (8c), only the linearized δL differential equation is obtained using the Clohessy-Wiltshire-Hill equations, while the linearized differential equations of in-plane angle ψ and out-of-plane angle θ are derived from the full formation angular momentum expression along with Euler's equation. Compared to the regulation problem, these differential equations are non-autonomous and depend explicitly on time through $L_{\text{ref}}(t)$. This greatly complicates the stability analysis of any feedback control law.

Let the charge product variation δQ be the control signal. The Coulomb regulation feedback control is then modified to incorporate a time-varying $L_{\text{ref}}(t)$ term. The new feedback control law for Coulomb reconfiguration is given as

$$\delta Q = \frac{m_1 m_2 L_{\text{ref}}^2(t)}{(m_1 + m_2)\,k_c}(-C_1\delta L - C_2\delta\dot{L}) \tag{9}$$

The constants C_1 and C_2 are the position and velocity feedback gains. Incorporating this feedback law in to the δL differential equation in Eq. (8c) yields the following closed-loop separation distance dynamics:

$$\delta\ddot{L} + \ddot{L}_{\text{ref}} - 2\Omega L_{\text{ref}}\dot{\psi} + (C_1 - 9\Omega^2)\delta L + C_2\delta\dot{L} = 0 \tag{10}$$

It can be observed that the linearized equations in Eq. (8a) – (8c) depend on the mean orbit rate Ω which has a very small value at GEO. In order to eliminate the numerical issues that might arise while integrating due to the small Ω value, the following normalization transformation is employed to make these equations independent of Ω.

$$\mathrm{d}\tau = \Omega\mathrm{d}t \tag{11a}$$

$$(*)' = \frac{\mathrm{d}(*)}{\mathrm{d}\tau} = \frac{1}{\Omega}\frac{\mathrm{d}(*)}{\mathrm{d}t} \tag{11b}$$

The orbit rate independent form of the linearized equations in Eq. (8a) – (8c) are written

as

$$\theta'' + \frac{2L'_{\text{ref}}}{L_{\text{ref}}}\theta' + 4\theta = 0 \tag{12a}$$

$$\psi'' + \frac{2L'_{\text{ref}}}{L_{\text{ref}}}\psi' + \frac{2}{L_{\text{ref}}}\delta L' - \frac{2L'_{\text{ref}}}{L^2_{\text{ref}}}\delta L + \frac{2L'_{\text{ref}}}{L_{\text{ref}}} + 3\psi = 0 \tag{12b}$$

$$\delta L'' + L''_{\text{ref}} - 2L_{\text{ref}}\psi' + (\tilde{C}_1 - 9)\delta L + \tilde{C}_2\delta L' = 0 \tag{12c}$$

where $\tilde{C}_2 = (C_2/\Omega)$ and $\tilde{C}_1 = (C_1/\Omega^2)$ are non-dimensionalized feedback gains. These equations show that the out-of-plane motion θ is decoupled from the charge product term δQ and separation distance variation δL. Therefore, it is not possible to control the out-of-plane motion using charge control in this linearized analysis. This is in accordance with the axially symmetric, slender rigid body dynamics[15] and the physically connected tether dynamics.[12] However, the in-plane motion ψ is coupled to the δL motion in the form of a driving force and hence, requiring a coupled in-plane attitude and separation distance stability analysis.

3 Stability Analysis

With time varying $L_{\text{ref}}(t)$, the equations of motion are linear and time dependent. Rosenbrock[20] shows that the linear time-dependent system given by $\dot{\boldsymbol{x}} = A(t)\boldsymbol{x}$ is asymptotically stable if the frozen system for each t is stable and the rate of change of $A(t)$ is very small. Reference 20 also establishes a bound for $A'(t)$ when $A(t)$ is in the control canonical form. The stability of the 2-craft Coulomb tether formation with varying reference length is analyzed using this method. The coupled δL and ψ equations in Eq. (12b) – (12c) are written in the state space form as

$$\begin{pmatrix} \psi' \\ \psi'' \\ \delta L' \\ \delta L'' \end{pmatrix} = \underbrace{\begin{bmatrix} 0 & 1 & 0 & 0 \\ -3 & -\frac{2L'_{\text{ref}}}{L_{\text{ref}}} & \frac{2L'_{\text{ref}}}{L^2_{\text{ref}}} & -\frac{2}{L_{\text{ref}}} \\ 0 & 0 & 0 & 1 \\ 0 & 2L_{\text{ref}} & 9 - \tilde{C}_1 & -\tilde{C}_2 \end{bmatrix}}_{A(t)} \begin{pmatrix} \psi \\ \psi' \\ \delta L \\ \delta L' \end{pmatrix} + \underbrace{\begin{pmatrix} 0 \\ -\frac{2L'_{\text{ref}}}{L_{\text{ref}}} \\ 0 \\ -L''_{\text{ref}} \end{pmatrix}}_{d(t)} \tag{13}$$

The square matrix in the above equation is $A(t)$ and the time dependency in this matrix is due to the terms L_{ref} and L'_{ref}. The stability of the system greatly depends on the rate at which L_{ref} is varied. The rate of change of reference length L'_{ref}, can be chosen according to the mission requirement or design. Of interest is how large L'_{ref} can be while still guaranteeing stability. From Eq. (13), it can be observed that there is a state independent term $d(t)$ which only depends on the specified rate of change of reference length (L'_{ref}). This term in the equation of motion will lead to a steady state offset as long as L_{ref} is time varying. The analytical expression for the steady state offset is given as follows

$$\begin{pmatrix} \psi_{\text{offset}} \\ \delta L_{\text{offset}} \end{pmatrix} = \begin{pmatrix} -\frac{2L'_{\text{ref}}}{3L_{\text{ref}}} + \frac{2L'_{\text{ref}}L''_{\text{ref}}}{3(-9+3\tilde{C}_1)L^2_{\text{ref}}} \\ \frac{L''_{\text{ref}}}{(-9+3\tilde{C}_1)} \end{pmatrix} = \begin{pmatrix} -\frac{2\dot{L}_{\text{ref}}}{3\Omega L_{\text{ref}}} + \frac{2\dot{L}_{\text{ref}}\ddot{L}_{\text{ref}}}{3\Omega(-9\Omega^2+3\tilde{C}_1)L^2_{\text{ref}}} \\ \frac{\ddot{L}_{\text{ref}}}{(-9\Omega^2+3C_1)} \end{pmatrix} \tag{14}$$

Before fixing the limits for L'_{ref}, the values for gains are chosen such that the $A(t)$ matrix is Hurwitz at any given time t. This does not guarantee stability for a time varying system, but this is a necessary step for the Rosenbrock stability conditions. In the regulation problem the feedback gains were expressed in terms of scaling factor c and α. Since this work is an extension of the regulation problem, the same scaling factor for the gains are chosen. They can be written as

$$\tilde{C}_1 = c \tag{15}$$

and

$$\tilde{C}_2 = \alpha\sqrt{c - 9} \tag{16}$$

The characteristic equation of the $A(t)$ matrix is given by

$$\lambda^4 + (\tilde{C}_2 + 2\frac{L'_{\text{ref}}}{L_{\text{ref}}})\lambda^3 + (\tilde{C}_1 + 2\tilde{C}_2\frac{L'_{\text{ref}}}{L_{\text{ref}}} - 2)\lambda^2 + (3\tilde{C}_2 - 22\frac{L'_{\text{ref}}}{L_{\text{ref}}} + 2\tilde{C}_1\frac{L'_{\text{ref}}}{L_{\text{ref}}})\lambda$$
$$+ 3(\tilde{C}_1 - 9) = 0 \quad (17)$$

Let $k = L'_{\text{ref}}/L_{\text{ref}}$ be a time varying coefficient which is determined through the chosen reference separation time history $L_{\text{ref}}(t)$. With this simplification the characteristic equation of $A(t)$ becomes

$$\lambda^4 + (\tilde{C}_2 + 2k)\lambda^3 + (\tilde{C}_1 + 2\tilde{C}_2 k - 2)\lambda^2 + (3\tilde{C}_2 - 22k + 2\tilde{C}_1 k)\lambda + 3(\tilde{C}_1 - 9) = 0 \tag{18}$$

To ensure stability, roots of the characteristic equation should have negative real parts (Hurwitz matrix). This requirement is satisfied using the Routh-Hurwitz stability criterion. Based on this criterion it is established that $\tilde{C}_1$ should have a value greater than 9 and the range of possible values for k and α for certain fixed $\tilde{C}_1$ is shown in Figure 3. The shaded region illustrates the possible values of k and α which guarantee that roots of the characteristic equation (i.e. the eigenvalues of the matrix $A(t)$) have negative real parts. It can be observed from Figure 3 that for $\tilde{C}_1 > 10$ there is no bounds on k when we are expanding the separation distance. But, for contracting or decreasing the separation distance (i.e. $-k$) we have a tight limit on k. The α value is fixed such that we have a maximum range of k. From Figures 3(b) and 3(c), the values of α are taken as 1.4 and 0.9 for the $\tilde{C}_1$ values of 12 and 14, respectively.

By satisfying the Routh-Hurwitz criterion, the eigenvalues of $A(t)$ at any fixed time t will always be in the left half of the plane. This is not sufficient to guarantee stability of the system. The sufficient condition is that rate of change of $A(t)$ be very small. Rosenbrock[20] established bounds for this rate of change and stated it as a theorem when $A(t)$ is in the control canonical form $(A_c(t))$. For the sake of continuity the theorem is stated here, but the reader should refer to Reference 20 for the detailed derivation of the theorem. Let the matrix R be defined as

$$R = SA_c^T + A_c S - S' + \eta I < 0 \tag{19}$$

$$(S_{ij}) = \sum_{k=1}^{n} \lambda_k^{i-1}\bar{\lambda}_k^{j-1} \tag{20}$$

(a) For $\tilde{C}_1 = 10$

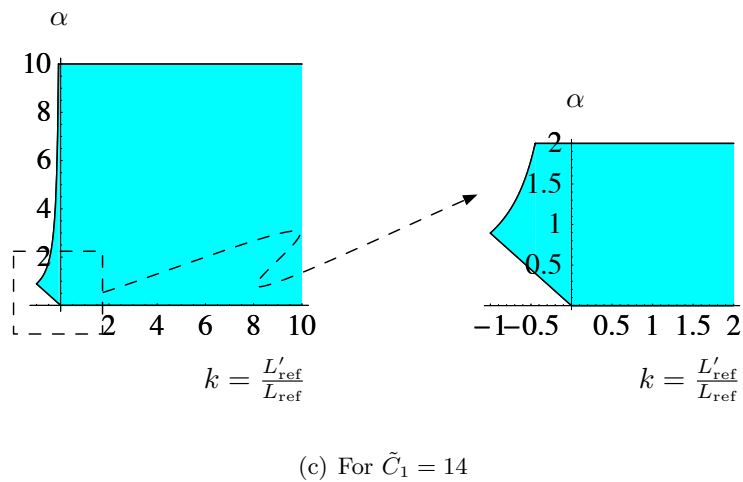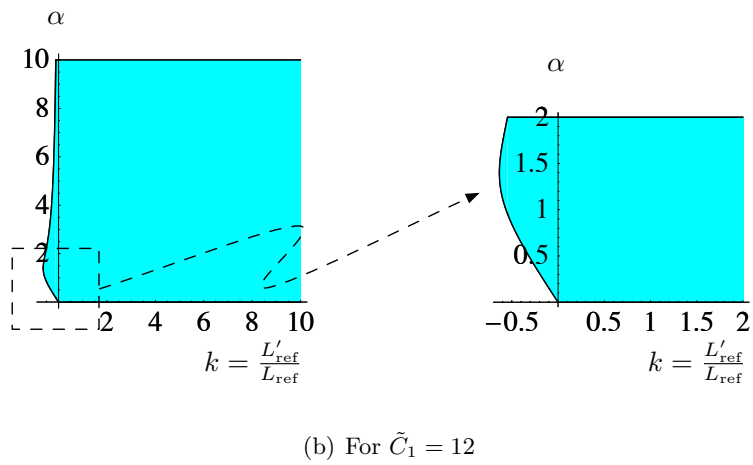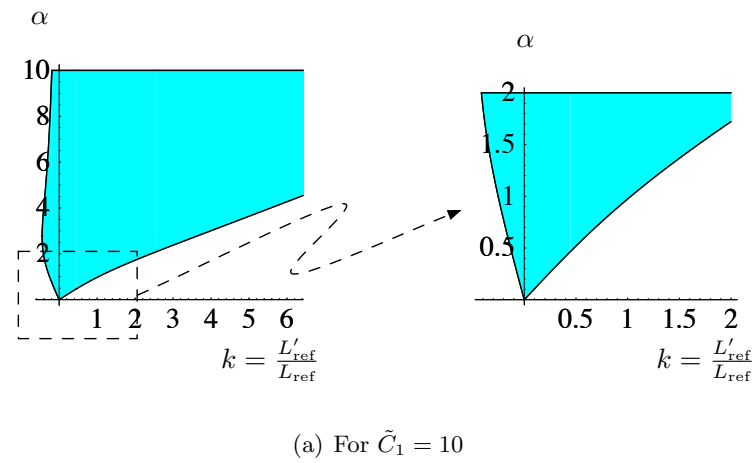(b) For $\tilde{C}_1 = 12$

(c) For $\tilde{C}_1 = 14$

Figure 3: Plots showing the regions that satisfy the Routh Hurwitz stability criterion.

where S_{ij} are the elements of the S matrix, λ_k and $\bar{\lambda}_k$ are the eigenvalues and its conjugate, S' is the derivative of S and $\eta > 0$ is some arbitrary constant. When all the eigen values of A_c are distinct and in the left half of the plane at any given instant of time, and R is negative definite throughout the maneuver, the system is asymptotically stable about $\boldsymbol{x} = 0$. For the 2-craft Coulomb tether problem, this requires the time varying reference separation distance $L_{\text{ref}}(t)$ to be carefully chosen so that the R is negative definite at all times. This theorem is based on the fact that for a matrix in the control canonical form, the eigenvalues are uniquely related to the elements of the matrix and hence, the bounds on the rate of change of the matrix can be replaced by bounds on the rate of change of the eigenvalues. Some more details about the S matrix are given in the following equation.

$$S = HH^* \tag{21}$$

where H is the is the eigenvector matrix and H^* is the transposed complex conjugate of H. The matrix H is defined as

$$H = \begin{bmatrix} 1 & 1 & \cdots & 1 \\ \lambda_1 & \lambda_2 & \cdots & \lambda_n \\ \lambda_1^2 & \lambda_2^2 & \cdots & \lambda_n^2 \\ \vdots & \vdots & \ddots & \vdots \\ \lambda_1^{n-1} & \lambda_2^{n-1} & \cdots & \lambda_n^{n-1} \end{bmatrix} \tag{22}$$

Studying the characteristic equation in Eq. (18), note that if $L'_{\text{ref}}(t)$ is chosen such that the coefficient $k = L'_{\text{ref}}/L_{\text{ref}}$ is constant, then the eigenvalues of $A_c(t)$ are also constant. For this special case the Rosenbrock stability conditions on the rate of change of $A(t)$ are trivially satisfied, and the overall stability is determined through the Routh-Hurwitz stability conditions. However, having a constant k coefficient is not a practical maneuver because it requires exponential expansion or contraction.

The $A(t)$ matrix in Eq. (13) is not in the control canonical form, but it can be transformed in a control canonical form using a similarity transformation $\boldsymbol{\xi} = T\boldsymbol{x}$ which yields the differential vector equation

$$\boldsymbol{\xi}' = A_c(t)\boldsymbol{\xi} \tag{23}$$

It should be noted that the characteristic equation of the transformed matrix $A_c(t)$ is the same as the original matrix $A(t)$. Hence, the values of gains chosen earlier will keep the eigenvalues in the left half plane. For this transformed matrix we can establish the bounds on L_{ref} and L'_{ref} which guarantee that the matrix L remains negative definite. The transformed states $\boldsymbol{\xi}$ are linear combinations of the original states $\boldsymbol{x}$. Therefore, if the transformed states are stable then the original states are also stable. The control canonical form of the matrix $(A_c(t))$ for the given matrix $A(t)$ can be easily written by observing the characteristic equation. It is given by

$$A_c(t) = \begin{bmatrix} 0 & 1 & 0 & 0 \\ 0 & 0 & 1 & 0 \\ 0 & 0 & 0 & 1 \\ -3(\tilde{C}_1 - 9) & -(3\tilde{C}_2 - 22k + 2\tilde{C}_1 k) & -(\tilde{C}_1 + 2\tilde{C}_2 k - 2) & -(\tilde{C}_2 + 2k) \end{bmatrix} \tag{24}$$
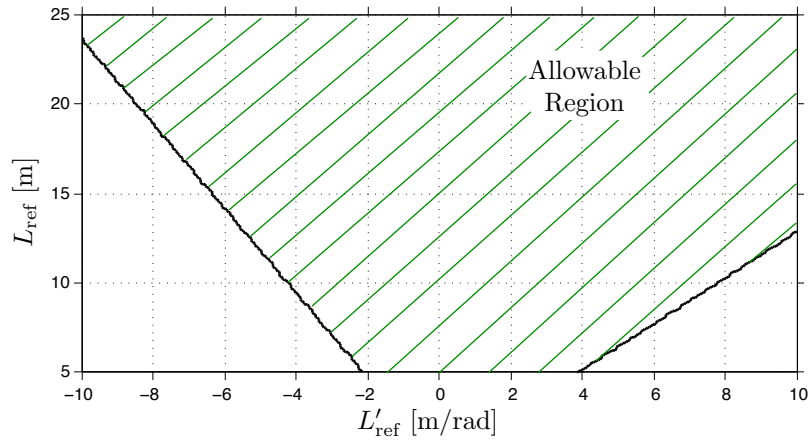
(a) For $\tilde{C}_1 = 12$ and $\alpha = 1.4$
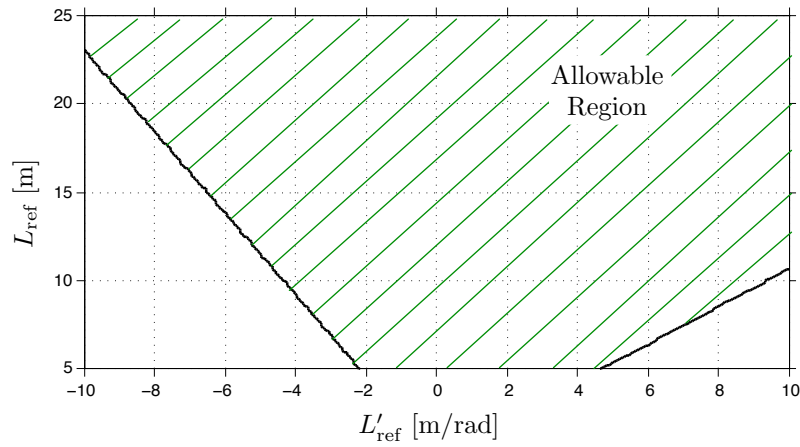
(b) For $\tilde{C}_1 = 14$ and $\alpha = 0.9$

Figure 4: Plots showing the regions that satisfy the Routh Hurwitz stability criterion and Rosenbrock bounds.

Because $A_c(t)$ is a 4×4 matrix, analytically finding the expression for eigenvalues and using them in the inequality in Eq. 19 is very challenging. The resulting expressions are too complex to be insightful. Instead the feasible values of L_{ref} and L'_{ref} that satisfies the inequality in Eq. 19 for the chosen values of $\tilde{C}_1$ and α are identified numerically. These feasible values are shown in Figure 4. The plots can be used to specify the reference trajectory $L_{\text{ref}}(t)$. Kulla[21] has developed a critical limit for the ratio $L'(t)/L(t)$ which guarantees stability for a tethered two-craft system. This critical limit is given as

$$L'(t)/L(t) = \dot{L}(t)/(\Omega L(t)) \leq 0.75 \tag{25}$$

This limit comes from a trigonometric constraint while balancing the Coriolis forces by the gravity gradient forces. The identified feasible values of L_{ref} and L'_{ref} for the current two craft virtual tether problem have linear constraint boundaries similar to the Kulla critical limit. The Coulomb tether problem is significantly different as a virtual tether allows both tension and compression, and the stability depends on the feedback gains. In comparison, the classical nadir-pointing tether reconfiguration problem requires tension at all times and only depends on the length rate $\dot{L}$.

4 Numerical Simulation

To illustrate the performance and stability of Coulomb tether reconfiguration maneuvers, the following numerical simulations are performed. The simulation parameters that used are listed in Table 1. The initial attitude values are set to $\psi = 0.1$ radians and $\theta = 0.1$ rad. The separation length error (Coulomb tether length error) is $\delta L = 0.5$ meters. All initial rates are set to zero through $\dot{\psi} = \delta\dot{L} = \dot{\theta} = 0$. Two sets of maneuvers, expanding the Coulomb tether formation from 25m to 35m in 1.8 days and contracting the formation from a separation distance of 25m to 15m, are shown.

Table 1: Input Parameters Used in Simulation

| Parameter	Value	Units
m_1	150	kg
m_2	150	kg
k_c	8.99×10^9	$\frac{\text{Nm}^2}{\text{C}^2}$
Ω	7.2915×10^{-5}	rad/sec
$\delta L(0)$	0.5	m
$\psi(0)$	0.1	rad
$\theta(0)$	0.1	rad

The Coulomb tether performance is simulated in two different manners. First the linearized spherical coordinate differential equations are integrated. This simulation illustrates the charge control performance operating on the linearized dynamical system. Second, the exact nonlinear equations of motion of the deputy satellites are solved using the same charge feedback control, and compared to the performance of the linearized dynamical system. The

nonlinear deputy equations are given through Cowell's equations

$$\ddot{\boldsymbol{r}}_1 + \frac{\mu}{r_1^3}\boldsymbol{r}_1 = \frac{k_c}{m_1}\frac{Q}{L(t)^3}(\boldsymbol{r}_1 - \boldsymbol{r}_2) \tag{26a}$$

$$\ddot{\boldsymbol{r}}_2 + \frac{\mu}{r_2^3}\boldsymbol{r}_2 = \frac{k_c}{m_2}\frac{Q}{L(t)^3}(\boldsymbol{r}_2 - \boldsymbol{r}_1) \tag{26b}$$

where $\boldsymbol{r}_1 = \boldsymbol{r}_c + \boldsymbol{\rho}_1$ and $\boldsymbol{r}_2 = \boldsymbol{r}_c + \boldsymbol{\rho}_2$ are the inertial position vectors of the the masses m_1 and m_2, while $L = \sqrt{(\boldsymbol{r}_2 - \boldsymbol{r}_1)\cdot(\boldsymbol{r}_2 - \boldsymbol{r}_1)}$. The vector $\boldsymbol{r}_c$ denotes the position of the formation center of mass or chief location. The gravitational coefficient μ is defined as $\mu \approx GM_e$. After integrating the motion using inertial Cartesian coordinates, the separation distance L, as well as the in-plane and out-of-plane angles ψ and θ, are computed in post-processing using the exact kinematic transformation.
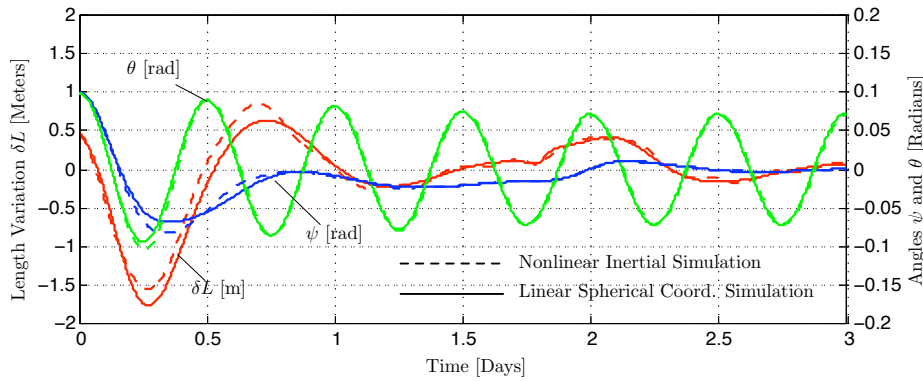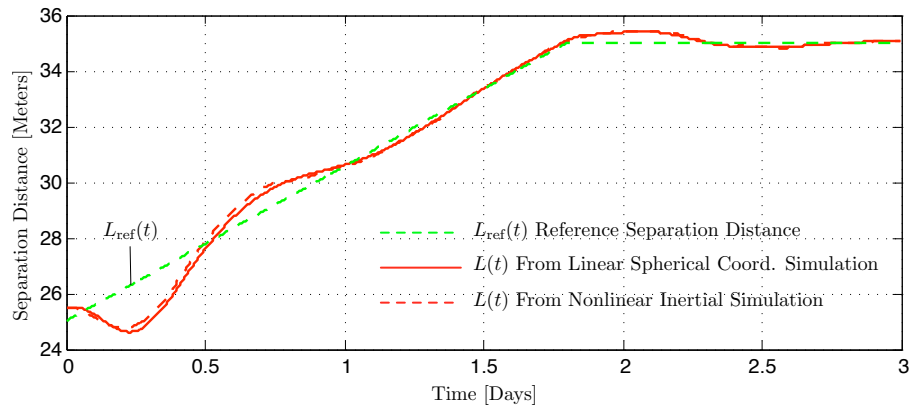

(a) Time histories of length variation δL, in-plane rotation angle ψ, and out-of-plane rotation angle θ.
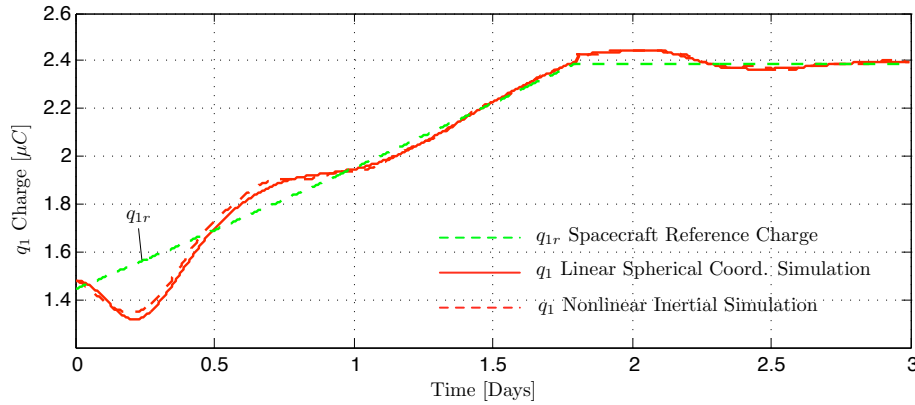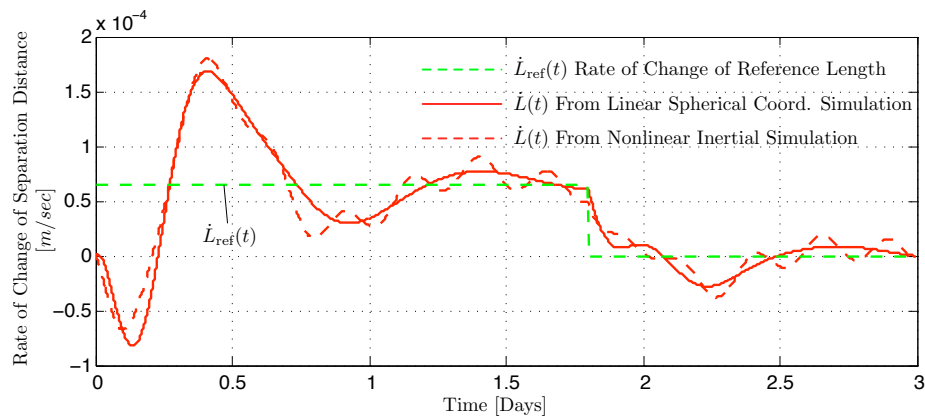

(b) Spacecraft charge time histories

Figure 5: Simulation results for expanding the spacecraft separation distance from $25\,m$ to $35\,m$ in 1.8 days. The feedback gains are $\tilde{C}_1 = 12$ and $\alpha = 1.4$.

Figure 5(a) shows the Coulomb tether motion for increasing the separation distance from 25m to 35m in the linearized spherical coordinates $(\psi, \theta, \delta L)$, along with the full nonlinear
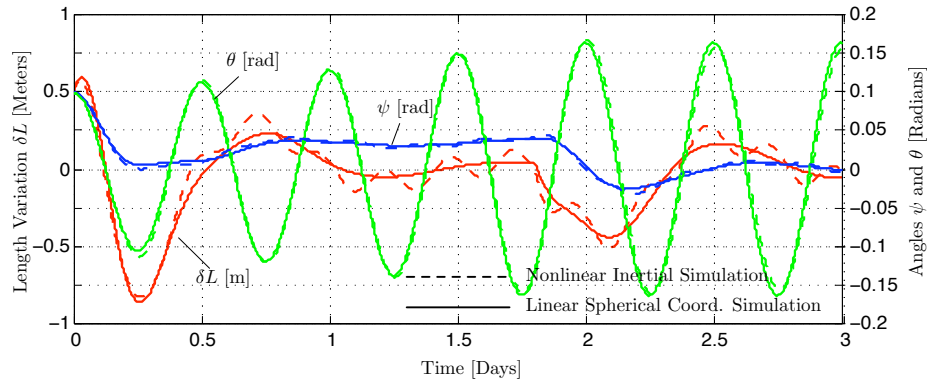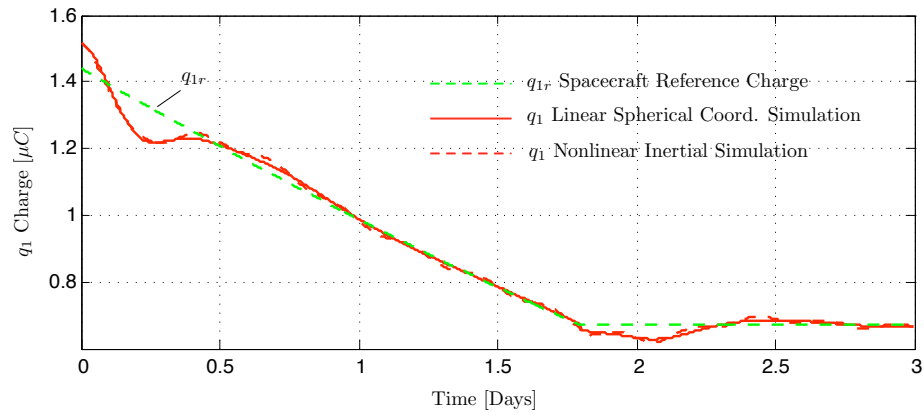
(a) Time histories of separation distance.

(b) Time histories of rate of change of separation distance

Figure 6: Simulation results for expanding the spacecraft separation distance from $25\,m$ to $35\,m$ in 1.8 days. The feedback gains are $\widetilde{C}_1 = 12$ and $\alpha = 1.4$.

(a) Time histories of length variation δL, in-plane rotation angle ψ, and out-of-plane rotation angle θ.

(b) Spacecraft charge time histories

Figure 7: Simulation results for contracting the spacecraft separation distance from 25 m to 15 m in 1.8 days. The feedback gains are $\tilde{C}_1 = 12$ and $\alpha = 1.4$.

spherical coordinates shown as dotted lines. The expansion is done in 1.8 days and this corresponds to a constant L'_{ref} of 0.88. After 1.8 days, the L'_{ref} is zero and the formation is allowed to stabilize about the final separation distance. The feedback gains are $\tilde{C}_1 = 12$ and $\alpha = 1.4$. With the presented charge feedback law, both the yaw motion ψ and the separation distance deviation δL converge to zero. By stabilizing the δL state to zero, the in-plane rotation $\psi(t)$ also converges to zero. As expected, the pitch motion $\theta(t)$ was a stable sinusoidal motion, decoupled from the controlled in-plane orbital motion. Further, Figure 5(a) shows that the nonlinear simulation closely follows the linearized simulation, validating the linearizing assumption and illustrating robustness to the unmodelled dynamics. Since L'_{ref} is constant, there is no steady state offset for δL and the offset for ψ is very small (order of 10^{-2} rad) and hence, not visible in the graph.

Figure 5(b) shows the spacecraft control charge q_1 (on craft 1) for both the linearized and full nonlinear simulation models. Both are converging to the reference value pertaining to the static equilibrium at each instant of time. Note that the deviation from the value of reference charges is small, justifying the linearization assumptions used. The magnitude of the control charges is in the order of micro-Coulomb which is easily realizable in practice using charge emission devices. The charge on craft 2 will be equal and opposite to the charge on craft 1.

In order to illustrate how well the system is tracking the prescribed reference trajectory $L_{\mathrm{ref}}(t)$, the time histories of separation distance $L(t)$ and the time histories of rate of change of separation distance $\dot{L}(t)$ are shown in Figure 6(a) and Figure 6(b), respectively. Figure 6(a) shows that the reference separation distance $(L_{\mathrm{ref}}(t))$ increases linearly until 1.8 days before settling to a constant value and both the linear and inertial nonlinear simulations track the reference separation distance closely. Figure 6(b) illustrates that the rate of change of the reference separation distance $(\dot{L}_{\mathrm{ref}}(t))$ is a discrete step change. In the linear and inertial nonlinear simulations the formation is assumed to be static to begin with and hence, their rate of change of separation distance $(\dot{L}(t))$ are zero initially. But they converge with the reference rate $\dot{L}_{\mathrm{ref}}(t)$ within 1.2 days. A faster convergence can be achieved by replacing the sharp corners of the reference rate (infinite reference acceleration) with a smooth polynomial function or spline (finite reference acceleration).

Figure 7(a) and Figure 7(b) show Coulomb tether motion and charge time histories for decreasing the separation distance from 25m to 15m. Contractions are more challenging because the angular momentum will cause to destabilize the in-plane attitude motion. The maneuvers must be performed slow enough to allow the gravity gradient to maintain stability. Again the maneuver is done in 1.8 days which means L'_{ref} is -0.88 and the gains are same as above expansion maneuver. These two sets of maneuvers are repeated for the gain values $\tilde{C}_1 = 14$ and $\alpha = 0.9$ and, Figure 8 and Figure 9 illustrate their time histories. It can be observed from these two graphs that even though the system is stable, the performance could potentially be improved by tuning the feedback gains.

5 Conclusions

A charge feedback control law for reconfiguring a 2-craft Coulomb tether formation with time varying length is given. The 2-craft system forms a simple virtual Coulomb structure where the electrostatic force replaces the physical tether cable. Previous work only considered stabilizing a static structure with a fixed length. This paper discusses an expanded
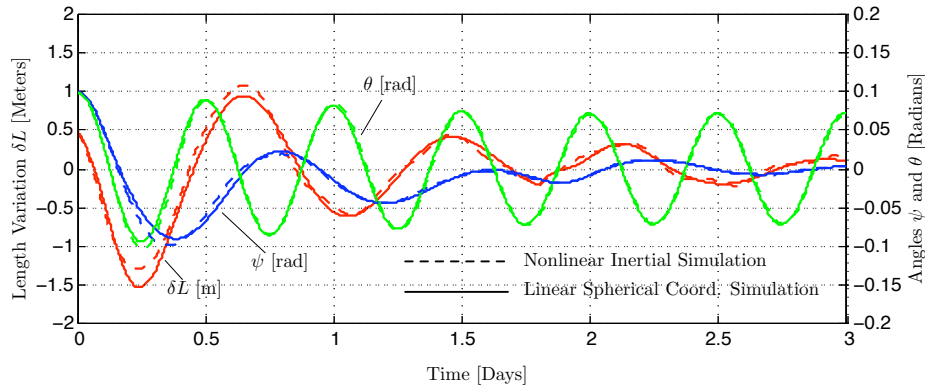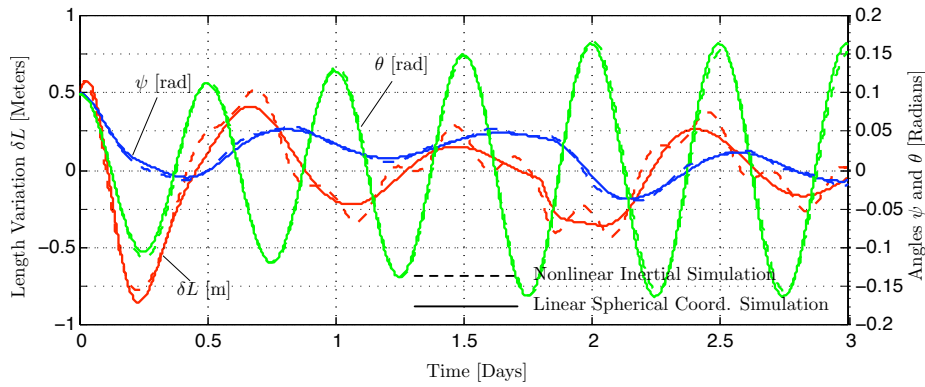
(a) Time histories of length variation δL, in-plane rotation angle ψ, and out-of-plane rotation angle θ.
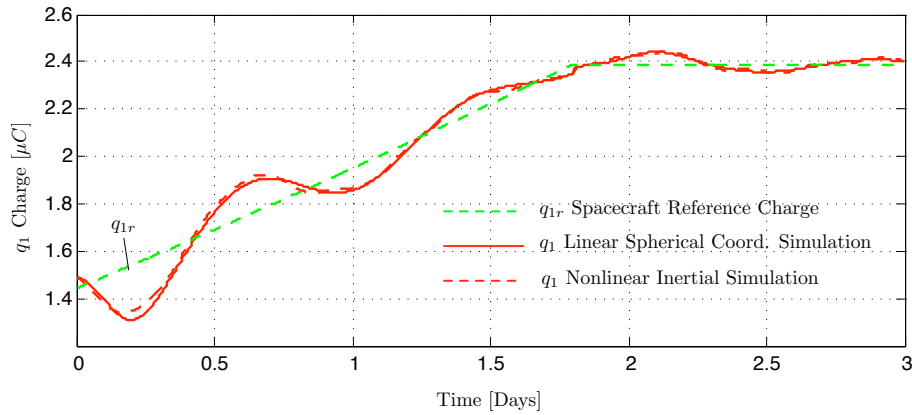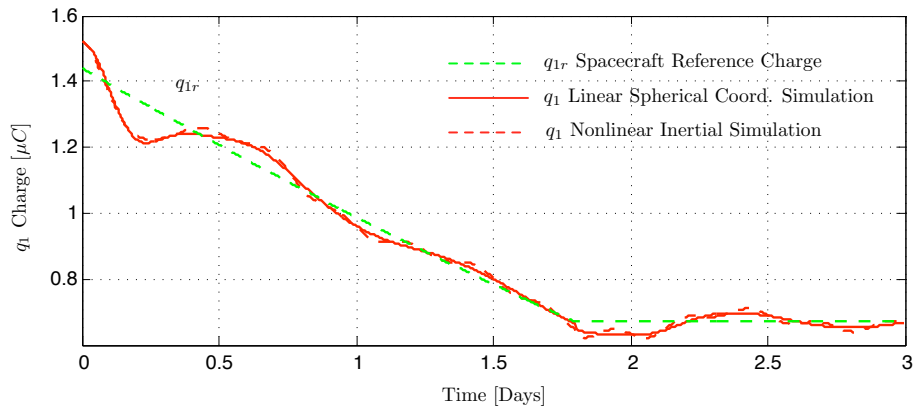

(b) Spacecraft charge time histories

Figure 8: Simulation results for expanding the spacecraft separation distance from $25\,m$ to $35\,m$ in 1.8 days. The feedback gains are $\tilde{C}_1 = 14$ and $\alpha = 0.9$.

(a) Time histories of length variation δL, in-plane rotation angle ψ, and out-of-plane rotation angle θ.

(b) Spacecraft charge time histories

Figure 9: Simulation results for contracting the spacecraft separation distance from $25\,m$ to $15\,m$ in 1.8 days. The feedback gains are $\tilde{C}_1 = 14$ and $\alpha = 0.9$.

feedback control law which allows for the Coulomb tether length to vary with time. During these maneuvers care is taken to ensure that the gravity gradient torque is still sufficient to stabilize the in-plane attitude of the nadir pointing formation. The stability regions for expanding and contracting the formation are established through linearization of the motion and by applying criteria developed by Rosenbrock for linear time-varying systems. Contracting the virtual structure is more difficult to perform while guaranteeing stability. The system angular momentum will cause any in-plane angular motion to increase with decreasing tether length. The magnitude of the local gravity gradient limits the rate at which the separation distance can be reduced. In contrast, expanding the virtual structure length is easier because the angular momentum helps contain in-plane rotation. The out-of-plane motion of the craft is decoupled from the in-plane motion with the linearized dynamics, and not controllable with the Coulomb forces. Numerical simulations of the full nonlinear motion are carried out to illustrate the results and compare the linearized performance predictions to the actual nonlinear system response.

Acknowledgment

References

[1] KING, LYON B., PARKER, GORDON G., DESHMUKH, SATWIK, ET AL., "Spacecraft Formation-Flying using Inter-Vehicle Coulomb Forces", Tech. rep., NASA/NIAC, January 2002, http://www.niac.usra.edu.

[2] KING, LYON B., PARKER, GORDON G., DESHMUKH, SATWIK, ET AL., "Study of Interspacecraft Coulomb Forces and Implications for Formation Flying", *AIAA Journal of Propulsion and Power*, Vol. 19, No. 3, May–June 2003, pp. 497–505.

[3] SCHAUB, HANSPETER, PARKER, GORDON G., and KING, LYON B., "Challenges and Prospect of Coulomb Formations", *AAS John L. Junkins Astrodynamics Symposium*, College Station, TX, May 23-24 2003, Paper No. AAS-03-278.

[4] MULLEN, E. G., GUSSENHOVEN, M. S., HARDY, D. A, ET AL., "SCATHA Survey of High-Level Spacecraft Charging in Sunlight", *Journal of the Geophysical Sciences*, Vol. 91, Feb. 1986, pp. 1474–1490.

[5] NICHOLSON, DWIGHT R., *Introduction to Plasma Theory*, Krieger, 1992.

[6] GOMBOSI, TAMAS I., *Physics of the Space Environment*, Cambridge University Press, 1998.

[7] BERRYMAN, JOHN and SCHAUB, HANSPETER, "Static Equilibrium Configurations in GEO Coulomb Spacecraft Formations", *AAS/AIAA Space Flight Mechanics Meeting*, Copper Mountain, Colorado, Jan. 2005, paper No. AAS 05-104.

[8] BERRYMAN, J. and SCHAUB, H., "Analytical Charge Analysis for 2- and 3-Craft Coulomb Formations", *AAS/AIAA Astrodynamics Specialist Conference*, Lake Tahoe, Aug. 2005, paper No. 05-278.

[9] PETTAZZI, LORENZO, KRUGER, HANS, THEIL, STEPHAN, ET AL., "Electrostatic Forces for Satellite Swarm Navigation and Reconfiguration.", Tech. rep., European Space Agency, 2006.

[10] IZZO, DARIO and PETTAZZI, LORENZO, "Self-Assembly of Large Structures in Space Using Intersatellite Coulomb Forces", *56th International Astronautical Congress*, Fukuoka, Japan, Oct. 17–21 2005, paper IAC-06-C3.4/D3.4.07.

[11] NATARAJAN, ARUN and SCHAUB, HANSPETER, "Linear Dynamics and Stability Analysis of a Two-Craft Coulomb Tether Formation", *AIAA Journal of Guidance, Control, and Dynamics*, Vol. 29, No. 4, Jul.–Aug. 2006, pp. 831–839.

[12] BELETSKY, VLADIMIR V. and LEVIN, EVGENII M., *Dynamics of Space Tether Systems*, American Astronautical Society Publications, San Diego, California., 1993.

[13] XU, D. M., MISRA, A. K., and MODI, V. J., "Three-Dimensional Control of the Shuttle Supported Tethered Satellite System During Retrieval.", *Proc. of the 3rd VPI&SU/AIAA Symp. on Dynamics and Control of Large Flexible Spacecraft*, Blacksburg, VA, USA, Jun. 1981, (pp. 453–469).

[14] MODI, V. J., CHANG-FU, G., MISRA, A. K., ET AL., "On the Control of the Space Shuttle Based Tethered Systems", *Acta Astronautica*, Vol. 9, 1982, pp. 437–443.

[15] SCHAUB, HANSPETER and JUNKINS, JOHN L., *Analytical Mechanics of Space Systems*, AIAA Education Series, Reston, VA, October 2003.

[16] CLOHESSY, W. H. and WILTSHIRE, R. S., "Terminal Guidance System for Satellite Rendezvous", *Journal of the Aerospace Sciences*, Vol. 27, No. 9, Sept. 1960, pp. 653–658.

[17] HILL, GEORGE WILLIAM, "Researches in the Lunar Theory", *American Journal of Mathematics*, Vol. 1, No. 1, 1878, pp. 5–26.

[18] SCHAUB, HANSPETER and PARKER, GORDON G., "Constraints of Coulomb Satellite Formation Dynamics: Part I – Cartesian Coordinates", *Journal of Celestial Mechanics and Dynamical Astronomy*, 2004, submitted for publication.

[19] SCHAUB, HANSPETER and KIM, MISCHA, "Orbit Element Difference Constraints for Coulomb Satellite Formations", *AIAA/AAS Astrodynamics Specialist Conference*, Providence, Rhode Island, Aug. 2004, paper No. AIAA 04-5213.

[20] ROSENBROCK, H. H., "The Stability of Linear Time Dependent Control Systems", *J. of Electronics and Control*, Vol. 15, 1968, pp. 73–80.

[21] KULLA, P., "Dynamics of Tethered Satellites", *Proc. Symp. on Dynamics and Control of Non-Rigid Spacecraft*, Frascati, Italy, 1976, (pp. 349–354).